

NASA CR-166,405

NASA CONTRACTOR REPORT 166405

NASA-CR-166405
19820025560

FOR INFORMATION

NOT TO BE USED FOR THE BOOK

Study of Fatigue Durability of Advanced Composite
Materials under Conditions of Accelerated Loading

Hsiuan-Ming Shih

LIBRARY COPY

SEP 23 1982

LANGLEY RESEARCH CENTER
LIBRARY, NASA
HAMPTON, VIRGINIA

CONTRACT NAS2-10061
September 1982



NF02360

NASA

NASA CONTRACTOR REPORT 166405

Study of Fatigue Durability of Advanced Composite
Materials under Conditions of Accelerated Loading

Hsiuan-Ming Shih
Advanced Research and Applications Corporation
1223 E. Arques Ave.
Sunnyvale, CA 94086



National Aeronautics and
Space Administration

Ames Research Center
Moffett Field, California 94035

N82-33436 #

ABSTRACT

The effect of temperature on the tension-tension fatigue life of the $[\pm 45^\circ]_{2s}$ T300/5208 graphite/epoxy angle-ply laminate system has been investigated in an effort to develop an acceptable and reliable method of accelerated loading. Typical $S\text{-}\log_{10} N$ curves were determined experimentally at 25°C , 75°C , and 115°C . The time-temperature superposition principle was employed to find the shift factors of uniaxial fatigue strength, and a general linear equation of $S\text{-}\log_{10} N$ for shifting purpose was established. The combined techniques of cyclic creep measurements and optical microscopy upon fatigue failure allow some assessment of the possible physical basis of $S\text{-}\log_{10} N$ curve shifting. It was concluded that before fatigue failure, the laminates at all test temperatures and stress levels undergo a unique damage mechanism during fatigue loading. As a result of the present investigations, it is concluded that an accelerated loading method is feasible and can be developed.

INTRODUCTION

The exceptionally high strength-to-weight and stiffness-to-weight ratios of advanced polymer-matrix, fiber-reinforced composites, such as the graphite/epoxy system, make them one of the outstanding primary structural materials in the aeronautical and automotive industries. Despite many efforts in the past to understand their mechanical performance, there still remains important technical questions to be answered before extensive usage of composite materials will occur. One such question concerns the long-term durability of their mechanical performance, such as fatigue, upon exposure to temperature and moisture of varying environments. A general guideline, based on some fatigue failure criterion of fiber-reinforced composite, will be helpful for design purposes. However, due to the large variety of laminations, it is almost impossible to obtain such a guideline through experiments only.

Recently, Hashin and Rotem^{1,2} developed with success a fatigue failure theory for a number of off-axis and angle-ply laminates based upon the fatigue failure criterion of constituting laminae. The theory can be used to predict the fatigue life of more complex laminates once the basic fatigue behaviors, such as those in longitudinal (fiber) direction, in transverse direction, and in in-plane shear, etc., are known for a particular composite system. Rotem and Nelson³ predicted the fatigue life of multi-directional symmetric-balanced laminates, $(0^\circ, \pm\theta, 0^\circ)$ and found good agreement between the predicted and experimentally determined values. This success initiated a study to find a feasible accelerated loading method for composite systems, such that the prediction of long-term fatigue life at lower temperatures (and/or lower moisture content) can be made reliably and accurately from the short-life test results at high temperature (and/or high moisture content). This method assumed that the time-temperature superposition principle, which is well-established in some classes of viscoelastic materials,⁴ also holds for polymeric materials in a composite system. Yeow and coworkers,⁵ showed, from tensile creep tests on a unidirectional GR/EP composite system, that the matrix-dominated properties of composites are time and temperature dependent and their

master curves of compliance or modulus could be produced by shifting the experimental results at higher temperatures to that at reference temperatures. A reasonable agreement between a WLF type equation⁴ and the determined shift factor was obtained for temperatures above T_g . Rotem and Nelson³ obtained the shift factors of both static and fatigue strengths in transverse and in-plane shear directions of the GR/EP composite with limited data.

It is thus clear that a good fatigue failure criterion and a reliable and feasible accelerated loading method will be needed in order to make a breakthrough in predicting long-term mechanical performances of more general composite systems. It is, therefore, the purpose of the present work to: (1) develop more extensive fatigue data at various temperatures and (2) determine the feasibility of the accelerated loading method. Tension-tension fatigue tests with load control on $[\pm 45^\circ]_{2s}$ T300/5208 composite laminates were carried out to determine reliable $S\text{-}\log_{10} N$ curves and the shift factors were obtained. Mean strain and strain amplitude values were monitored simultaneously to track down possible damage accumulation. These results, when combined with optical microscopy, will allow some assessment of the feasibility of the accelerated loading method and its physical basis.

Throughout this work, we report only the experimentally measured strength properties in axially loading direction symmetric to $[\pm 45^\circ]_{2s}$ laminates. No attempt was made to calculate in-plane shear strength by the conventional equation

$$\tau_{12} = \sigma_x/2 \quad (1)$$

where τ_{12} is in-plane shear stress and σ_x is the applied stress in the loading direction. The shear strength, τ_{12} , was not calculated because of the influence of transverse stress on the in-plane shear strength in the $[\pm 45^\circ]_{2s}$ laminates.^{6,7} There are still some questions as to the best test method and the laminate lay-up which would give the real in-plane shear strength of a given composite system.^{8,9,10}

ANALYTICAL FORMULATION OF SHIFT FUNCTIONS

According to Rotem and Nelson,³ the uniaxial fatigue strength, σ^u , of a composite laminate at any temperature can be determined through a shifting equation

$$\begin{aligned}\sigma^u(T) &= a^S(T) \sigma^S(T_0) f(N,T) \\ &= a^S(T) \sigma^S(T_0) a^f(T) f(N,T_0)\end{aligned}\quad (2)$$

when keeping load ratio, R, and cyclic frequency, n, constant, and

$$\begin{aligned}a^S(T) &= \text{static strength shift factor} \\ \sigma^S(T_0) &= \text{static strength at reference temperature} \\ a^f(T) &= \text{fatigue strength shift factor} \\ f(N,T), f(N,T_0) &= \text{fatigue functions at test and reference} \\ &\quad \text{temperatures, respectively.}\end{aligned}$$

The shift process according to equation (2) was described in detail in Rotem and Nelson's³ paper and will not be repeated here. Interested readers can refer to their paper.

Care must be exercised when using the equation to find the shift factors $a^S(T)$ and $a^f(T)$. The problems are two-fold. First, from equation (2):

$$f(N,T) = a^f(T) f(N,T_0) = \frac{\sigma^u}{a^S(T) \sigma^S(T_0)} \quad (2a)$$

If $S - \log_{10} N$ (or $\sigma^u - \log_{10} N$; σ^u and S are used interchangeably throughout the paper) curves are linear, $f(N,T)$ will have the form of:

$$f(N,T) = A(T) + B(T) \log_{10} N \quad (3)$$

Rotem and Nelson's³ expression then implies

$$a^f = \frac{A(T_0) + B(T_0) \log_{10} N}{A(T) + B(T) \log_{10} N} \quad (4)$$

In this case, a^f will be a function of T and N , not a function of T only. This will make the shifting process difficult. Secondly, the choice of the static strength value presents some problems. If the static strength value obtained by static loading ($\sim \frac{1}{4}$ cycle) is plotted on the $S\text{-}\log_{10} N$ diagram, most of experimental data^{11,12} show a situation presented in Figure (1). Now, if the shifting process is carried out to bring two curves at higher temperatures, T_1 and T_2 , to that at T_0 by a^s , equal to $\sigma_A(T_0)/\sigma_A(T)$, and a^f , the rotation of higher temperature curves, it will be impossible for them to form a single master curve, which is the key to predicting fatigue life at any temperature. These problems bring about a new approach of choosing a "static" strength parameter and formulating a new general linear equation of $S\text{-}\log_{10} N$ suitable for all the shifting purposes. This is described as follows:

If the least-square fitted form of $S\text{-}\log_{10} N$ is linear, then it can be written as

$$\sigma^u(T) = a(T) + b(T) \log_{10} N \quad (5)$$

at any temperature. Let's identify the extrapolated fatigue strength parameter of $a(T)$ at $N = 1$ at given temperature as σ_e^u .

This quantity is a uniquely determined value as long as the $S\text{-}\log_{10} N$ curve is obtained experimentally and least-square fitted. Equation (5) can be normalized with respect to σ_e^u and rewritten as

$$\begin{aligned} \frac{\sigma^u}{\sigma_e^u} &= f(N, T) \\ &= 1 + \frac{b(T)}{\sigma_e^u} \log_{10} N \\ &= 1 + B(T) \log_{10} N \end{aligned} \quad (6)$$

The shift factors can then be determined from $\sigma_e^u(T)$'s and $B(T)$'s. Since the shifting process of $S\text{-}\log_{10} N$ curves is always associated with the direction of temperature shift, it is better to express the shift factors,

a^s and a^f , as a function of the directionality. The directionality is represented by

$$\Delta T = T_o - T \quad (7)$$

where T and T_o are the initial and final temperatures of shifting, respectively. a^s and a^f will have values which depend on the sign of ΔT . This dependence leads us to write a^s and a^f as a function of ΔT and they are defined, from equation (6), as

$$a^s(\Delta T) = \frac{\sigma_e^u(T_o)}{\sigma_e^u(T)} \quad (8)$$

$$a^f(\Delta T) = \frac{B(T_o)}{B(T)}$$

and

$$\begin{aligned} a^s(\Delta T < 0) &= 1/a^s(\Delta T > 0) \\ a^f(\Delta T < 0) &= 1/a^f(\Delta T > 0) \\ a^f, a^s &= 1 @ \Delta T = 0 \end{aligned} \quad (9)$$

Equation (6) can thus be expressed in terms of the shift factors in a more general form

$$\begin{aligned} \sigma_e^u(T+\Delta T) &= a^s(\Delta T) \sigma_e^u(T) \left[1 + a^f(\Delta T) B(T) \log_{10} N \right] \\ \text{or} \quad &= a^s(\Delta T) \sigma_e^u(T) f(N, T, \Delta T) \end{aligned} \quad (10)$$

when $\Delta T = 0$, i.e., in the case of no shifting, equation (10) is simply equation (7) itself. For $\Delta T \neq 0$, then the $S0 \log_{10} N$ curve at temperature T can be converted to that at T_o simply by substituting the appropriate values of a^s and a^f in equation (10). Because of this versatility, equation (10) will be used to analyze the present fatigue studies on $[\pm 45^0]_{2s}$ GR/EP laminates.

Finally, it is worthwhile to point out that the above treatment of the shift of $S\text{-log}_{10} N$ curves is purely mathematical. Its physical basis remains to be studied. Although the epoxy resin is viscoelastic and the concept of compliance or modulus shifting has been well established⁴ for various kinds of viscoelastic materials, the application of this concept to composites under fatigue loading still has to be verified. The shift of $S\text{-log}_{10} N$ can only be performed with reservation, since the similarity of fatigue damage accumulation mechanisms at various temperatures has not yet been established.

EXPERIMENTAL

The material used for this investigation was Thornel 300/NARMCO 5208 graphite/epoxy composite. The $[\pm 45^\circ]_{2s}$ angle-ply laminates of the composite were fabricated by Lockheed Missiles and Space Company from pre-impregnated tape purchased from NARMCO. NARMCO specifications of minimum tensile strength and average tensile modulus for the graphite fibers were 2.66 and 220 ~ 240 GPa, respectively. Consolidation of the lay-up of T300/5208 was effected in an autoclave at a pressure of 0.7 MPa (100 psig) and a temperature of 175°C for 120 ~ 130 minutes. The resulting panel had an average fiber volume of 65% and thickness of 0.12 cm. The dimensions of test specimens with fiberglass fabric end tabs are shown in Figure (2).

Tension-tension fatigue studies of the laminates were conducted at room environment by using an electrohydraulic, servo-controlled 10 M.T. (50 KiP) MTS^R testing system having a linear actuator. The fatigue tests were carried out in load control mode at a frequency of 10 HZ and $R = 0.1$ (ratio of minimum to maximum applied load). Test temperatures were 25°C, 75°C, and 115°C. All test specimens were kept at testing temperature for one hour prior to cyclic loading. Typical $S\text{-}\log_{10} N$ data were developed at each temperature. To evaluate the possible material degradation from cyclic creep behavior, the mean value of strain output was monitored during the test using a data acquisition system consisting of a Wang 6000 programmable calculator and Fluidyne Interfacing Instruments. Cyclic creep, ϵ_{cc} , is defined as

$$\epsilon_{cc} = \epsilon_m(t) - \epsilon_m(0) \quad (11)$$

where $\epsilon_m(t)$ and $\epsilon_m(0)$ denote mean strains at $t=t$ and $t=0$, respectively.

Test specimens which failed in fatigue were prepared for optical microscopy. The cross section of the specimen to be examined was cut 1.5 cm away from failure location. Since the failure location in $[\pm 45^\circ]_{2s}$ laminate is probabilistic, the choice would give a typical bulk micro-structure upon fatigue failure. Final stages of polishing were conducted using 3 μ , 1 μ and 0.25 μ diamond paste.

RESULTS AND DISCUSSION

Fatigue Studies

Figure 3 shows experimental results of maximum alternating stress (or fatigue strength), σ^u , versus cycles to failure, N , of the laminates at three different temperatures. Three or more specimens were tested at each stress level. The experimental data at each temperature were pooled together and least-square fitted. Table I shows the fitted parameters, a and b , of the linear equation

$$\sigma^u = a + b \log_{10} N$$

and the sample correlation coefficient, γ , and the standard error of the estimate, S_{yx} , of fittings for all test temperatures.

Table I

LEAST SQUARE ESTIMATES TO LINEAR
EQUATION OF $\sigma^u = a + b \log_{10} N$

Temp., °C	a, MPa	b	γ	S
25	171.45	-14.85	-0.990	1.87
75	143.96	-11.80	-0.995	0.93
115	113.43	- 6.97	-0.982	1.28

These results indicate that the fatigue strength, σ^u , of the laminate decreases to a possible limiting value as temperature increases for a given fatigue life. This is to be expected of a matrix-dominated laminate with a viscoelastic matrix. However, it is interesting to note that the fatigue sensitivity represented by b , the slope of S - $\log_{10} N$ curves, also decreases in absolute value as temperature increases. This result suggests that the $[\pm 45^\circ]_{2s}$ GR/EP laminate will have longer fatigue life at higher temperatures for applied stress levels below a certain value.

In the present case, this threshold value is about 68 MPa. Askins¹² also reported similar behavior of $[\pm 45^\circ]_{2s}$ SP 313 laminates under tension-tension fatigue of $f = 30$ HZ, $R = 0.1$. SP 313 composite is an alternative to T300/5208 for USAF fighter aircraft structures.

Figures 4 and 5 show cyclic creep measurements plotted as a function of normalized time, n/N , with stress level and temperature, respectively, as independent variables. Stress level and temperature are shown to have significant influence on cyclic creep. Increases in each of these parameters accelerate the rate of cyclic creep. Furthermore, all cyclic creep curves in both figures show the same characteristics, similar to those of metallic creep. Each curve consists of three stages: (1) transient (primary), (2) steady state (secondary), and (3) incipient failure (tertiary), where the specimen falls apart. By analogue to metallic creep, these results suggest that the cyclic creep of the laminate is due to the flow of epoxy resin matrix, at least up to the end of the second stage. There could also be an additional contribution to cyclic creep, especially in the final stage, due to the accumulation of ply cracks on the weakest positions in the interface of matrix and fiber. Whether the accumulation of ply cracks or the matrix flow dominates cyclic creep during fatigue is of interest in that this could determine the major degradation mechanism during fatigue. Once this is determined, the physical basis of shifting can be assessed. This will be discussed in the section reporting microscopy studies.

Shifting of S-log₁₀ N Curves

From Table I, the fitted equations of S-log₁₀ N data for the laminate after fatigue loading at three temperatures are:

$$\begin{aligned}\sigma^u &= 171.45 - 14.85 \log_{10} N, \text{ MPa @ } 25^\circ\text{C} \\ &= 143.96 - 11.80 \log_{10} N, \text{ MPa @ } 75^\circ\text{C} \\ &= 113.43 - 6.97 \log_{10} N, \text{ MPa @ } 115^\circ\text{C}\end{aligned}\quad (12)$$

The extrapolated fatigue strength at N = 1 are:

$$\begin{aligned}\sigma_e^u &= 171.45 \text{ MPa @ } 25^\circ\text{C} \\ &= 143.96 \text{ MPa @ } 75^\circ\text{C} \\ &= 113.43 \text{ MPa @ } 115^\circ\text{C}\end{aligned}$$

Therefore, equations (12) can be rewritten as

$$\begin{aligned}\sigma^u &= \sigma_e^u (A + B \log_{10} N) \\ &= 171.45 (1 - 0.087 \log_{10} N) \text{ @ } 25^\circ\text{C} \\ &= 143.96 (1 - 0.082 \log_{10} N) \text{ @ } 75^\circ\text{C} \\ &= 113.43 (1 - 0.061 \log_{10} N) \text{ @ } 115^\circ\text{C}\end{aligned}\quad (13)$$

where A = 1 and B is taken to be the normalized slope with respect to σ_e^u . Now, if taking the final temperature of shifting, T_o, is taken to be 25°C, then for shifting S-log₁₀ N curve at 75°C to 25°C (ΔT = -50°C),

$$a^s(\Delta T) = \sigma_e^u(25^\circ\text{C}) / \sigma_e^u(75^\circ\text{C}) = 1.19$$

$$a^f(\Delta T) = B(25^\circ\text{C}) / B(75^\circ\text{C}) = 1.06$$

and, similarly, for shifting S-log₁₀ N at 115°C to 25°C (ΔT = -90°C),

$$\begin{aligned}a^s(\Delta T) &= 1.51 \\ a^f(\Delta T) &= 1.43.\end{aligned}$$

When the $S\text{-log}_{10} N$ curves at 75°C and 115°C were shifted by the determined factors, a^s and a^f , to that at 25°C , the combined single curve of $S\text{-log}_{10} N$ is shown in Figure 6. This master curve summarizes all the experimental data on the uniaxial tension-tension fatigue studies of $\pm 45^{\circ}_{2s}$ GR/EP laminates. Figure 7 shows the result of the shift factors, a^s and a^f , plotted as a function of ΔT when $T_o = 25^{\circ}\text{C}$. Figures 6 and 7, together with the appropriate fatigue failure criterion, make possible the prediction of long-term fatigue life at lower temperatures from the short-time test results at higher temperatures for this type of laminate subject to similar fatigue loading conditions.

Microscopic Studies of Fatigue Failure

The primary objective of this section is to show the fatigue damage buildup and its distribution within the bulk laminate upon fatigue failure. Temperature and stress levels were changed to study their influences on fatigue damage buildup and distribution. It has been widely agreed that the degradation of the laminate under fatigue loading occurs in the matrix first. Damage in fibers is the result of matrix degradation. Therefore, it is reasonable to assume that the fatigue damage in this laminate is in the form of a large number of cracks forming and propagating in the matrix. Hahn¹³ reasoned that though interlaminar stresses induce delamination along the free edges, they didn't seem to influence the fatigue strength. Fatigue damage occurs when ply cracks form within each lamina. Therefore, the measurements of ply crack buildup and its distribution in the bulk laminate far from free edge zones will provide insights into the extent of fatigue damage and its dependences upon applied stress level and temperature.

Figures 8, 9 and 10 show typical micrographs of the laminate cross sections perpendicular to the loading direction at fatigue failure. Delamination caused by interlaminar stress concentrations^{14,15} at the free edges occurs in all cases. Therefore, for the sake of the measurement of ply crack developed in the bulk laminate, any crack or

delamination occurring within the free-edge affected zone was not counted. From the calculation of Wang and Crossman¹⁵ on interlaminar stresses for $[\pm 45^\circ]_{2s}$ laminates, this zone was taken to be 0.25 of the laminate half width measured from the edge. This choice eliminated possible confusion from the free-edge effect.

Table II is a list of ply crack density, ρ , defined as the number of ply cracks per unit area of cross section, with stress level and temperature as variables. Several conclusions can be drawn from the measurements and microscopic observations. They are:

1. At a given temperature, the average ply crack density is higher at lower stress levels than at higher stress levels.
2. For roughly the same fatigue life, ply crack density is higher at higher temperature. This is consistent with the assumption that fatigue damage occurs when ply crack forms. The larger the ply crack density, the greater the fatigue damage. Therefore, lower fatigue strength of the laminate at higher temperature leads to the same fatigue life as that at lower temperature with higher fatigue strength.
3. Given the same stress level, ply crack density is apparently not affected by temperature.
4. There is no correlation between the variation of ply crack density and that of the fatigue life at given stress level and temperature.
5. The distribution of ply cracks within the bulk laminate is macroscopically homogeneous. Ply cracks can occur either in the outer layer or in the central layers.
6. Delamination in the bulk laminate is present at higher temperatures (115°C). This may be due to the matrix relief of stress concentration caused by the penetrating ply crack.

Table III
MEASUREMENTS OF PLY CRACK DENSITY, ρ , AT FATIGUE FAILURE

Specimen No.	σ^u , MPa	N	ρ , #/cm ²	ρ_{av} , #/cm ²
25* -	32	121	2,540	125
	33	121	2,760	47
	34	121	2,090	47
				73
	36	92.8	199,000	146
	37	92.8	204,600	119
75* -	39	92.8	123,300	84
				116
	6	104	2,300	105
	7	104	2,520	84
	9	104	2,340	105
				98
	4	92.8	23,650	146
	20	69	6.8×10^6	146
	22	69	2.0×10^6	105
115*-	23	69	5.2×10^6	146
				133
	6	92.8	1,200	125
	7	92.8	3,100	165
	8	92.8	1,730	105
				132
	16	69	5.3×10^6	200
	17	69	1.4×10^6	188
	18	69	2.8×10^6	201
				196

* 25, 75, and 115 denote the test temperatures.

From the measurements of cyclic creep, it was found that increasing stress level increases cyclic creep strain at a given temperature. The increase was attributed to (a) the viscoelastic response of the matrix and (b) possible ply crack accumulation. However, the ply crack density was shown to be higher at lower stress levels. These contradictory results tend to suggest that there is no significant contribution of crack accumulation to the cyclic creep strain. The cyclic creep during tension-tension fatigue is mainly due to the viscoelastic flow of epoxy resin matrix.

With reference to the shifting of $S\text{-}\log_{10} N$ curves, the present results indicate that for all the test temperatures and stress levels of this study, ply cracks are uniformly present throughout the bulk laminate at fatigue failure and show the same dependence on the applied stress level. It was also learned that during tension-tension fatigue, the laminates creep mainly as a result of viscoelastic response of epoxy resin matrix. It is therefore concluded that there does exist a common physical rationale behind the shifting of $S\text{-}\log_{10} N$ curves of $[\pm 45^\circ]_{2s}$ GR/EP laminates under tension-tension fatigue loading. Thus, the scenarios of the laminate response under tension-tension fatigue at any tested temperature and stress level is as follows. During the fatigue loading, the laminate creeps with time. This is mainly due to the viscoelastic flow of epoxy resin matrix. At fatigue failure, there are ply crack formations throughout the bulk laminate. The density of ply crack depends on temperature and applied stress level.

CONCLUSIONS

1. $S\text{-log}_{10} N$ data of $[\pm 45^\circ]_{2s}$ GR/EP laminates show that increasing temperature decreases their fatigue strength, and fatigue sensitivity is significantly reduced as temperature is increased.
2. A general equation of $S\text{-log}_{10} N$ for shifting purpose was formulated in terms of the shifting factors which depend on the shifting direction. A master curve of $S\text{-log}_{10} N$ data for all test temperatures was established by using this equation.
3. From the results of cyclic creep measurements and optical microscopy, there is shown to be a physical basis for applying time-temperature superposition principle to $[\pm 45^\circ]_{2s}$ GR/EP laminates. It is the viscoelastic flow of matrix during fatigue, and ply crack formations at fatigue failure.

REFERENCES

1. Z. Hashin and A. Rotem, "A Fatigue Failure Criterion for Fiber Reinforced Materials," J. of Composite Materials, 7, 448 (1973).
2. A. Rotem and Z. Hashin, "Fatigue Failure of Angle Ply Laminates," AIAA Journal, 14, No. 7, 868 (1976).
3. A. Rotem and H. Nelson, "A Temperature Dependent Fatigue Failure Criterion for GR/EP laminates," NASA-TM-78538, 1978.
4. J. D. Ferry, "Viscoelastic Properties of Polymers," John Wiley Co., NY, 1961.
5. Y. T. Yeow, D. H. Morris and H. F. Brinson, "The Time-Temperature Behavior of a Unidirectional Graphite/Epoxy Composite," Virginia Polytechnic Institute Publication No. VPI-E-78-4, February 1978.
6. N. J. Wadsworth and J. Hutchings, "Transverse Properties of Carbon Fiber/Resin Composites," RAE Technical Report 67099 (1967).
7. T. A. Collings, "The Transverse Compressive Behavior of Unidirectional Carbon Fiber Reinforced Plastics," RAE Technical Report 72237 (1972).
8. B. W. Rosen, "A Simple Procedure for Experimental Determination of the Longitudinal Shear Modulus of Unidirectional Composites," J. Composite Materials, 6, 552 (1972).
9. H. T. Hahn, "A Note on Determination of the Shear Stress-Strain Response of Unidirectional Composites," J. Composite Materials, 7, 383 (1973).
10. C. C. Chamis and J. H. Sinclair, "Ten-degree Off-axis Test for Shear Properties in Fiber Composites," Experimental Mechanics, p. 339 (1977).
11. H. T. Sumsion and D. P. Williams, "Effects of Environment on the Fatigue of Graphite-Epoxy Composites," ASTM-STP-569, p. 226, 1975.
12. D. R. Askins, "Development of Engineering Data on Advanced Composite Materials," AFML-TR-77-151, September 1977.
13. T. Hahn, "Fatigue Behavior and Life Prediction of Composite Laminates," AFML-TR-78-43, April 1978.
14. R. B. Pipes and N. J. Pagano, "Interlaminar Stresses in Composite Laminates Under Uniform Axial Extension," J. Composite Materials, 4, 538 (1970).
15. A.S.D. Wang and Frank W. Crossman, "Some New Results on Edge Effect in Symmetric Composite Laminates," J. Composite Materials, 11, 92 (1977).

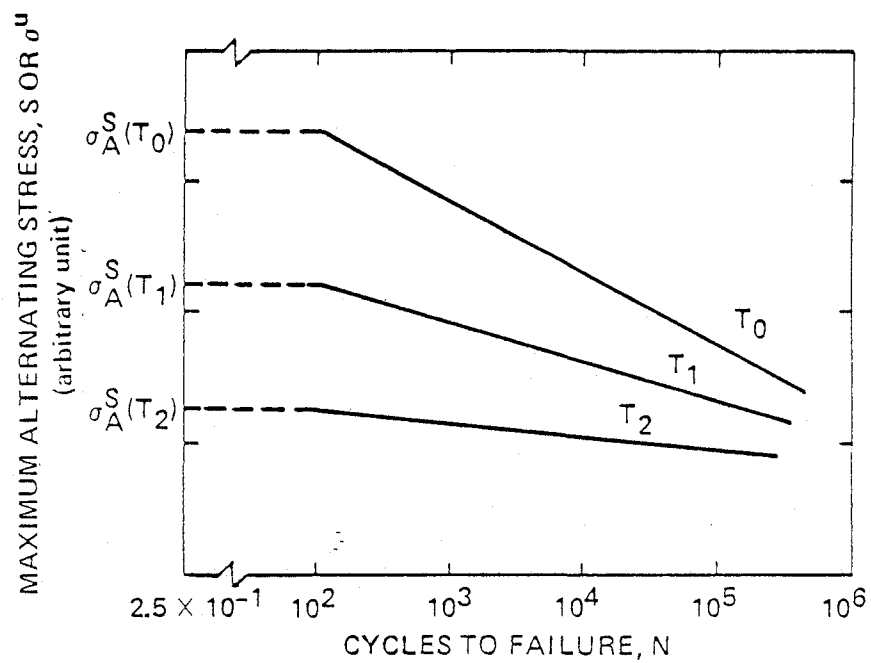


Figure 1. Schematic diagram of $S\text{-}\log_{10} N$ curves showing static strength together with fatigue data.

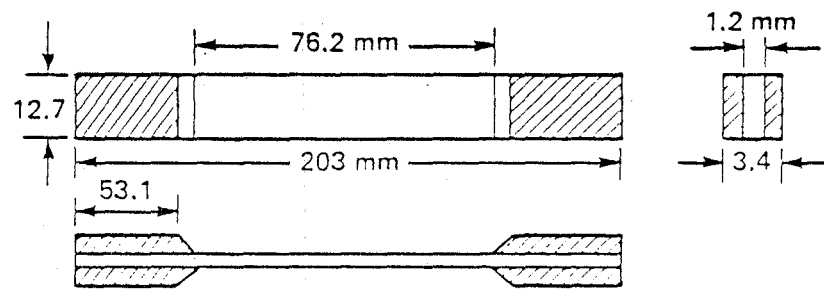


Figure 2. Specimen dimensions of $[\pm 45^\circ]_{2s}$ T300/5208 composite laminate with end tabs. Unit: mm.

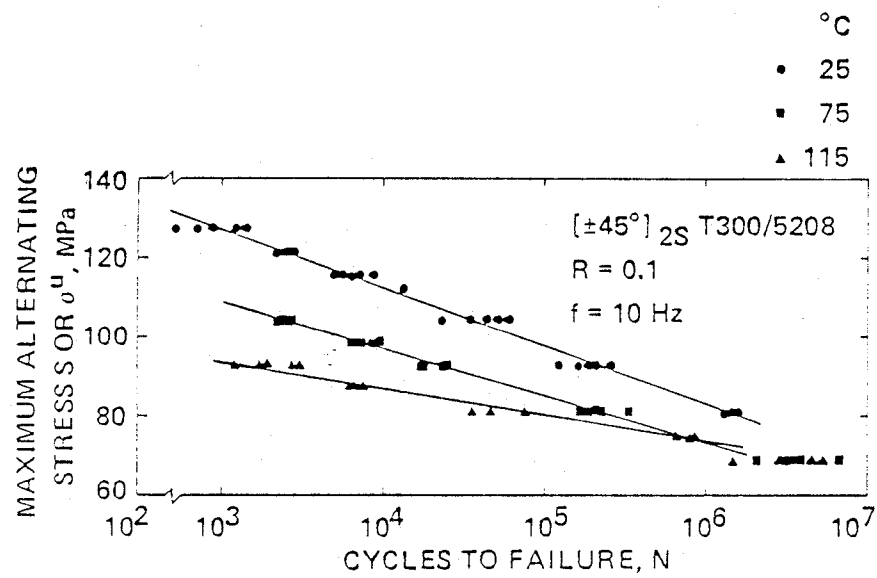


Figure 3. S- \log_{10} N data of $[\pm 45^{\circ}]_{2s}$ T300/5208 laminate
 at three different temperatures.

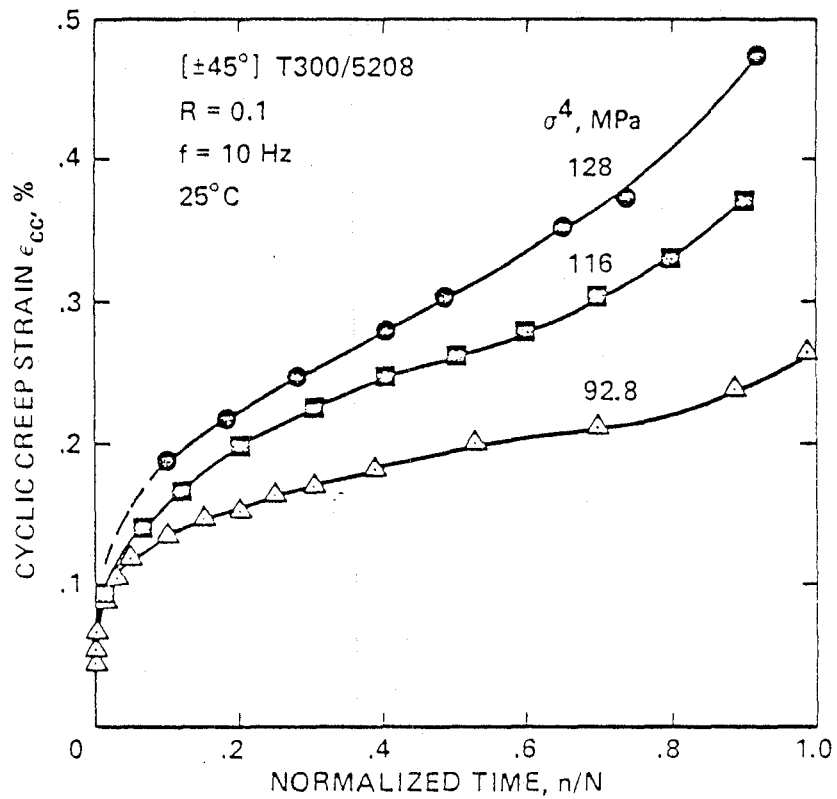


Figure 4. Measurements of cyclic creep strain plotted as a function of normalized time, n/N , at room temperature for different applied stress levels.

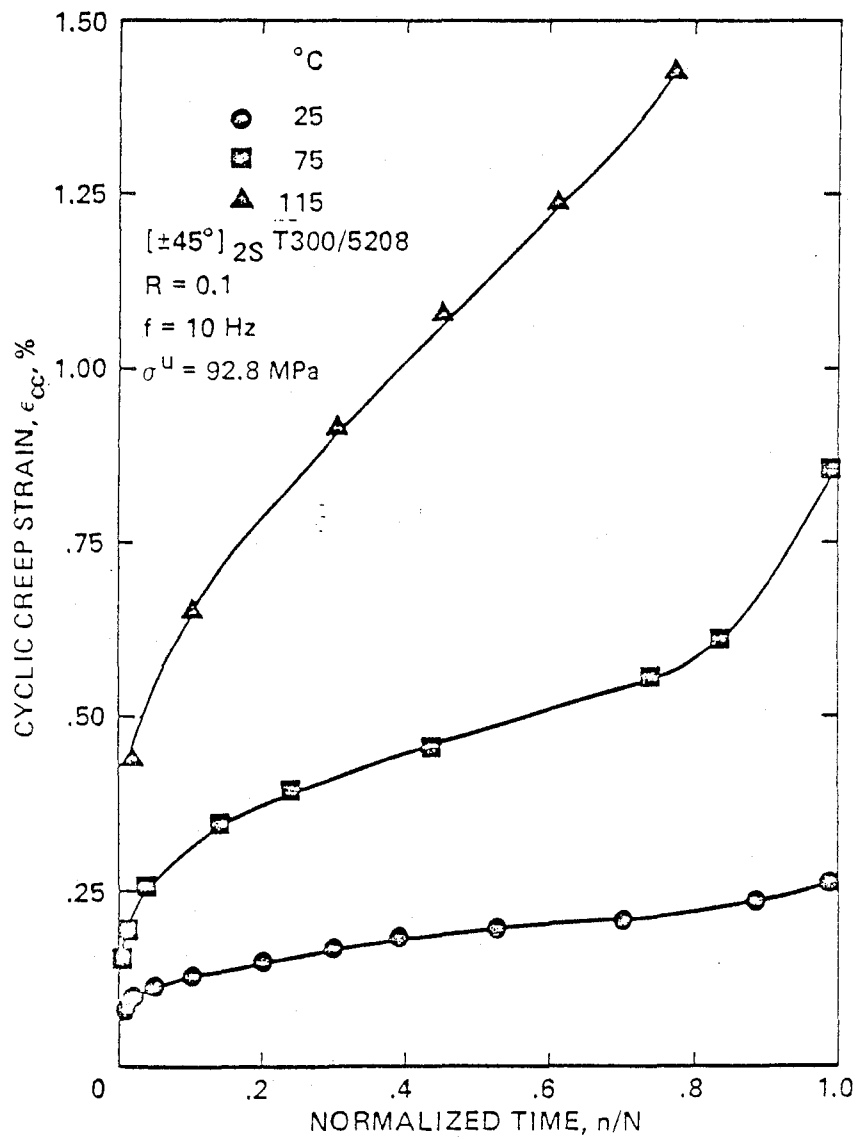


Figure 5. Measurements of cyclic creep strain plotted as a function of normalized time, n/N , at maximum alternating stress of 92.8 MPa for three different temperatures.

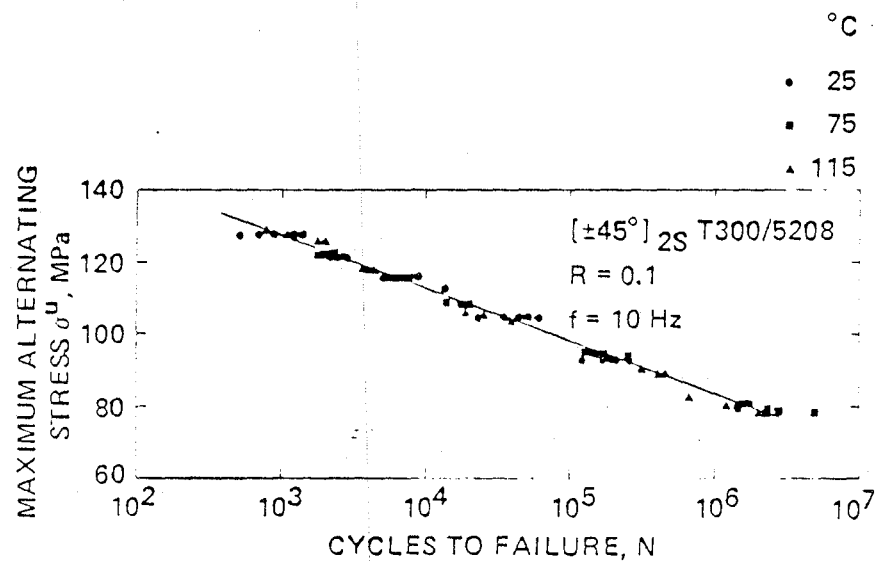


Figure 6. S- $\log_{10} N$ data at 25°C with the shifted data from 75°C and 115°C.

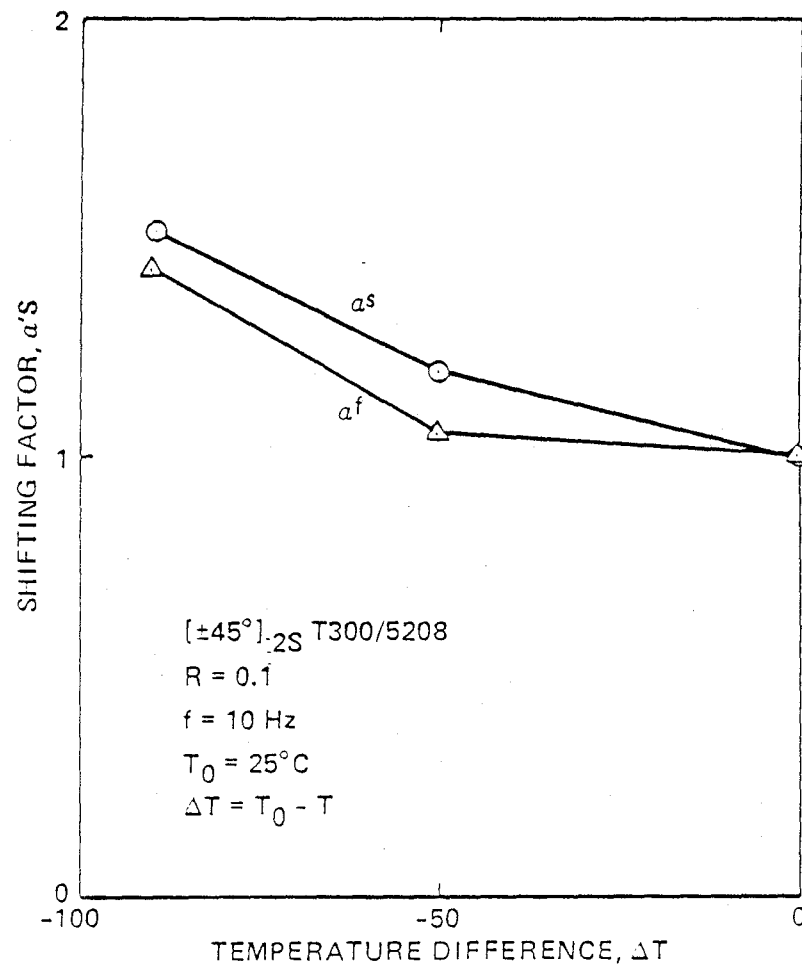
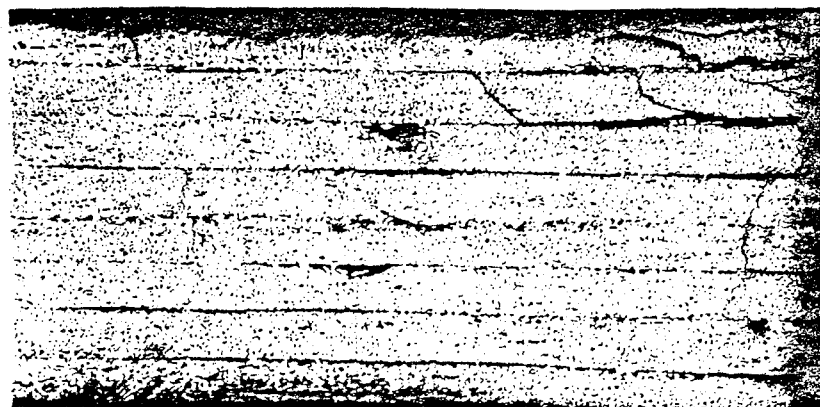
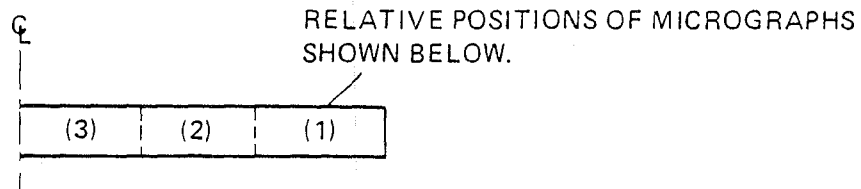
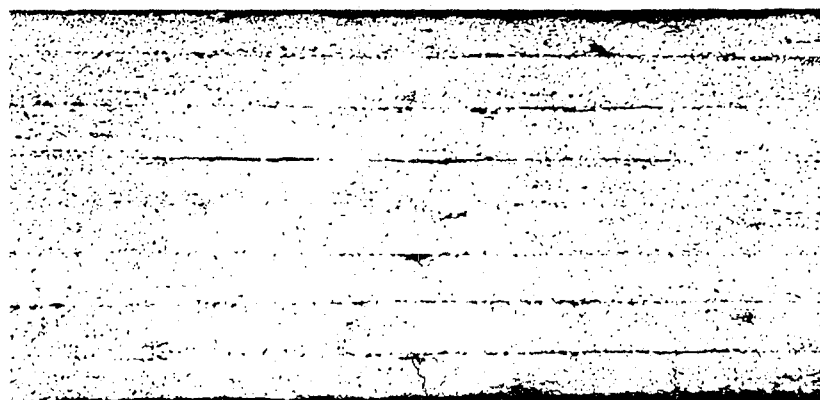


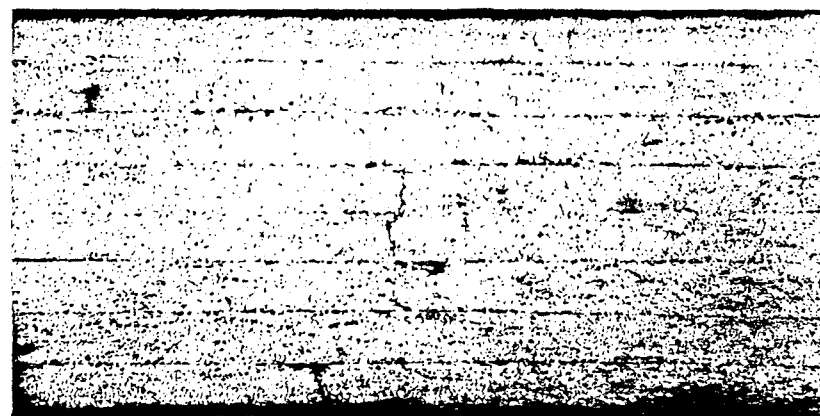
Figure 7. Shifting factors, a^s and a^f , of axial fatigue strength plotted as a function of temperature shift.



(1)



(2)

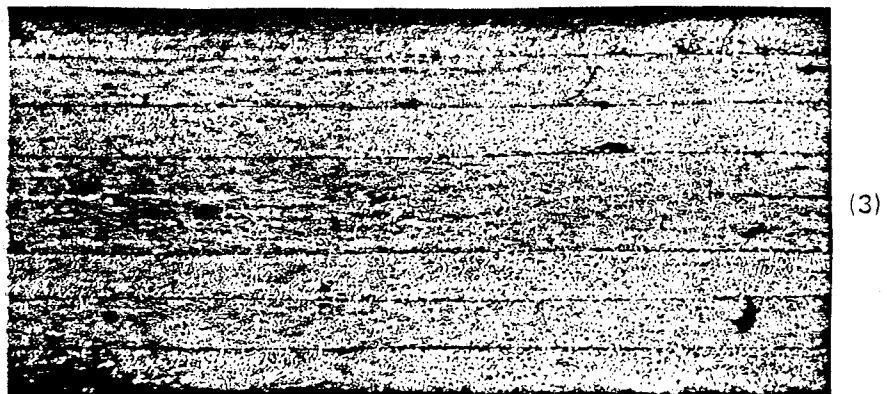
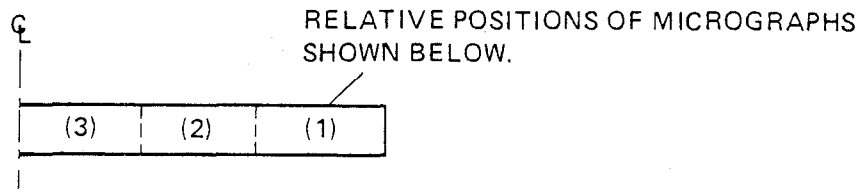


(3)

0.5 mm

Figure 8a. Optical micrographs showing ply crack buildup at fatigue failure.

25°C, $\tau^u = 92.8$ MPa



0.5 mm

Figure 8b. Optical micrographs showing ply crack buildup at fatigue failure.
75°C, $\sigma^u = 69$ MPa

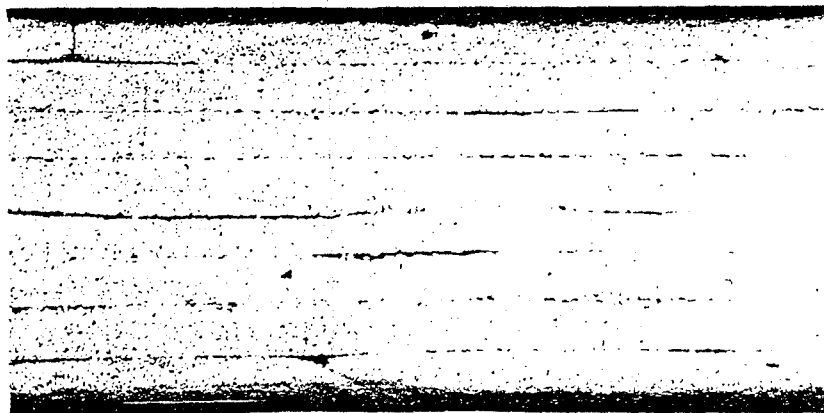
Q

RELATIVE POSITIONS OF MICROGRAPHS
SHOWN BELOW.

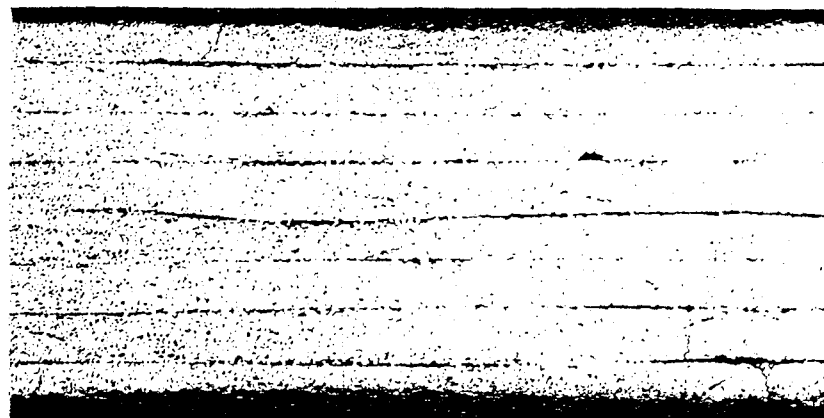
(3)	(2)	(1)
-----	-----	-----



(1)



(2)



(3)

0.5 mm

Figure 8c. Optical micrographs showing ply crack buildup at fatigue failure.

115°C, $\sigma^u = 69$ MPa

1. Report No. 166405	2. Government Accession No.	3. Recipient's Catalog No.	
4. Title and Subtitle STUDY OF FATIGUE DURABILITY OF ADVANCED COMPOSITE MATERIALS UNDER CONDITIONS OF ACCELERATED LOADING		5. Report Date October 1979	
		6. Performing Organization Code	
7. Author(s) Hsiuan-Ming Shih		8. Performing Organization Report No.	
9. Performing Organization Name and Address Advanced Research and Applications Corporation 1223 E. Arques Avenue Sunnyvale, CA 94086		10. Work Unit No.	
		11. Contract or Grant No. NAS2-10061	
12. Sponsoring Agency Name and Address National Aeronautics and Space Administration Washington, DC 20546		13. Type of Report and Period Covered Contractor Report	
		14. Sponsoring Agency Code	
15. Supplementary Notes Point of Contact: Dr. Howard G. Nelson, 230-4, NASA-Ames Research Center, Moffett Field, CA 94035, (415) 965-6137, FTS 448-6137			
16. Abstract The effect of temperature on the tension-tension fatigue life of the ($\pm 45^\circ$) _{2s} T300/5208 graphite/epoxy angle-ply laminate system has been investigated in an effort to develop an acceptable and reliable method of accelerated loading. Typical S-log ₁₀ N curves were determined experimentally at 25°C, 75°C, and 115°C. The time-temperature superposition principle was employed to find the shift factors of uniaxial fatigue strength, and a general linear equation of S-log ₁₀ N for shifting purposes was established. The combined techniques of cyclic creep measurements and optical microscopy upon fatigue failure allow some assessment of the possible physical basis of S-log ₁₀ N curve shifting. It was concluded that before fatigue failure, the laminates at all test temperatures and stress levels undergo a unique damage mechanism during fatigue loading. As a result of the present investigations, it is concluded that an accelerated loading method is feasible and can be developed.			
17. Key Words (Suggested by Author(s)) tension-tension fatigue, time-temperature superposition, cyclic creep, damage mechanism, accelerated testing.		18. Distribution Statement Unlimited STAR Category - 24	
19. Security Classif. (of this report) Unclassified	20. Security Classif. (of this page) Unclassified	21. No. of Pages 30	22. Price*

End of Document